KSCE Journal of Civil Engineering (2019) 23(2):821-832

DOI 10.1007/s12205-018-1990-6

Transportation Engineering

pISSN 1226-7988, eISSN 1976-3808
www.springer.com/12205

Impact of Connected and Automated Vehicles on Passenger Comfort of Traffic Flow with Vehicle-to-vehicle Communications

Yanyan Qin*, Hao Wang, and Bin Ran*****

Received December 17, 2017/Revised 1st: May 4, 2018, 2nd: July 19, 2018/Accepted October 1, 2018/Published Online December 17, 2018

Abstract

Extended transit time and increased consumer expectations arouse an interest in passenger comfort research. Few studies have been conducted on passenger comfort of Connected and Automated Vehicles (CAV) traffic flow, thereby leaving a research gap. This paper focuses on filling this research gap and evaluating CAV impact on passenger comfort from the traffic flow perspective. Specifically, optimal stability of traffic flow mixed with Manual Driven Vehicles (MDV) and CAV is desired to improve passenger comfort. For describing stability condition of the mixed traffic flow, in which multiple connected feedbacks of CAV exist with Vehicle-to-Vehicle (V2V) communications, local vehicular platoons with uniform structure are considered to be the optimization objective. Its stability charts with respect to equilibrium speeds and CAV feedback gains are calculated based on transfer function theory, thereby controlling CAV feedback gains for optimal stability. The CAV impact on the passenger comfort is evaluated under optimal control results of CAV feedback gains, by using numerical simulations under car-following models. It is indicated that stability optimization benefits passenger comfort of the mixed CAV traffic flow.

Keywords: *connected and automated vehicles, passenger comfort, traffic flow stability, transfer function, car-following models*

1. Introduction

In recent years, intelligent vehicular systems are rapidly developed, such as Adaptive Cruise Control (ACC) vehicles, and Cooperative Adaptive Cruise Control (CACC) vehicles. Soon afterwards, Connected and Automated Vehicles (CAV) are also developed in Vehicle-to-Vehicle (V2V) communication environment. These intelligent vehicular systems are desired to improve traffic flow operation from a microscopic perspective, thereby potentially benefiting traffic safety, road capacity, emissions, and passenger comfort. At the present stage, study on impacts of CAV on traffic flow dynamics is a hot topic in research fields of traffic flow theory and intelligent transportation systems (Mahmassani, 2016).

In previous studies, a lot of literatures focused on traffic safety (Lin *et al*., 2014), road capacity (Shladover *et al*., 2012), fuel consumption and emissions (Wang *et al*., 2015), and traffic flow stability (Talebpour and Mahmassani, 2016). However, studies on CAV impacts are not balanced. There are relatively small amount of literature conducted for the impact of CAV on passenger comfort. The passenger comfort is one of the important traffic flow characteristics, which has been interested in extended transit time and increased consumer expectations (Elbanhawi *et al*., 2015). It was indicated that people could influence manual drivers' driving speeds in terms of passenger comfort (Fleiter *et al*., 2010). In the case of CAV, the control system takes over manual drivers, while passengers are not changed. Passengers cannot affect CAV control systems when the vehicle is running on the road. Hence, the passenger comfort of CAV should be seriously considered before implementations in production vehicles.

Raimondi and Melluso (2008) proposed a cooperative scheme for CAV by using decentralized planning algorithm. Study results indicated that the low values of longitudinal and lateral accelerations were guaranteed to ensure comfort during vehicle's motion. Wu *et al*. (2009) proposed a car-following control model focused on passenger comfort. The passenger discomfort caused by longitudinal deceleration was removed by controlling the vehicle's acceleration. Experiments were also used to validate the compatibility with real cases. Moon *et al*. (2009) studied the design, tuning, and evaluation of the full-range ACC system, in which the collision avoidance was considered. Although the proposed ACC system was focused on improving safety, the control scheme was also designed taking the passenger comfort into consideration. Glaser *et al*. (2010) presented a maneuver-based trajectory-planning algorithm for CAV, which was tested on a simulator to show the improvement of passenger comfort.

*Ph.D. Student, School of Transportation, Jiangsu Key Laboratory of Urban ITS, Southeast University, Nanjing 210096, China; Dept. of Civil and Environment Engineering, University of Wisconsin–Madison, Madison, WI 53706, USA (E-mail: qinyanyan@seu.edu.cn)
**Professor, School of Transportation, Jiangsu Key Laboratory of Urban ITS, Jiangsu Province Collaborative Innovation Center of Modern Urban Traffic Technologies, Southeast University, Nanjing 210096, China (Corresponding Author, Email: haowang@seu.edu.cn)
***Professor, Dept. of Civil and Environment Engineering, University of Wisconsin–Madison, Madison, WI 53706, USA (E-mail: bran@wisc.edu)

Li *et al*. (2011) developed a novel ACC system to comprehensively address traffic issues including longitudinal ride comfort. In the presented ACC system, the model predictive control theory was utilized in the upper controller, while the hierarchical control architecture was employed in the lower controller. Dang *et al*. (2015) also used the model predictive control theory to propose a coordinated control algorithm for CACC vehicles focusing on enhancing the passenger comfort. Jayachandran and Krishnapillai (2013) studied the passive suspension system of vehicles and presented an optimization method for improving passenger comfort. Luo *et al*. (2015) presented an ACC system of hybrid electric vehicles. The nonlinear model predictive control was used for the development of the controller, based on which the position-based nonlinear longitudinal inter-vehicle dynamics model was proposed. Then experiments were carried out to indicate the enhancements of passenger comfort, safety, and fuel consumption. Lefèvre *et al*. (2016) proposed a learning-based framework for CAV speed control. In this study, a predictive controller was utilized to enforce comfort and safety constraints before outputting the final acceleration. Bellem *et al*. (2016) studied the driving style for CAV to improve passenger comfort. This article pointed out that maneuver-specific metrics were the essential components for the development of comfortable CAV driving.

However, these existing literatures about CAV impacts on the passenger comfort are not comprehensive. Elbanhawi *et al*. (2015) presented a review of state of the art of the passenger comfort in path planning for CAV. This research highlighted a research gap in the field of passenger comfort and pointed out that there is a need to evaluate passenger comfort in CAV traffic flow. In the recent study (Milakis *et al*., 2017), a review of literature and directions for future research of CAV were conducted. This study divided traffic flow efficiency, road capacity, travel choices, and passenger comfort into the first-order impacts of CAV. Based on the review of previous literatures, it shows that a critical knowledge gap about CAV impact on passenger comfort is still left to be future studied. Yang *et al*. (2017) also summarized the importance of examining the impact of CAV on passenger comfort from the traffic flow perspective.

It indicates that the passenger comfort is affected by fluctuations of vehicles' accelerations and speeds, which are closely related to traffic flow stability. At the equilibrium state of traffic flow, vehicles keep the constant speed and passengers have no uncomfortable feels. The relative poor passenger comfort occurs when vehicles depart from the equilibrium state under speed and acceleration disturbances. Therefore, it is interesting to study whether the stability optimization of CAV traffic flow can improve the passenger comfort. Unfortunately, little research has been conducted on this, based on the recent review studies (Hoogendoorn *et al*., 2014; Elbanhawi *et al*., 2015; Mahmassani, 2016; Milakis *et al*., 2017; Shladover, 2018; Yang *et al*., 2017). This paper presents an effort to fill this research gap.

In the case of stability analysis of CAV control under pure CAV environment, the stability methods for car-following models can be applied. Sau (2014) proposed a root locus method for stability analysis and design of cooperative car-following models under pure CAV environment. Jia and Ngoduy (2016) developed a cooperative car-following model with the combination of V2V and Vehicle-to-Infrastructure (V2I) communication. Then, they analyzed the stability of the proposed car-following models, based on which not only the vehicular flow stability is guaranteed, but also the shock waves are supposed to be smoothed. The recent study (Sun *et al.*, 2018) reviewed some stability analysis methods and their applicability to car-following models in conventional and connected environments. In their review, three types of models are considered: basic type car-following model, time-delayed type car-following model, and multi-anticipative/ cooperative car-following model. Moreover, the Lyapunov stability criterion, the Laplace transform based method, and the root locus method were employed for stability analysis. Although there are many studies on the stability analysis of car-following models, only a few studies focused on the stability analysis of the mixed traffic flow. Among them, the general method proposed by Ward (2009) is popular and widely extended, in which the microcosmic car-following models are used. Talebpour and Mahmassani (2016) first examined the stability question by extending the analytical approach developed by Ward (2009), and applying it in turn to systems with varying degrees of connected vehicles in one case, then autonomous vehicles in the other (Mahmassani, 2016). Moreover, Ngoduy (2013) also developed a macroscopic approach to analyze the traffic flow stability mixed with CACC vehicles. In the case of CAV, CAV can monitor multiple vehicles ahead under V2V communication environment. Based on this connected property, the feedback gains of CAV can be controlled for optimal stability situation of the mixed traffic flow, in order to improve passenger comfort. On the other hand, the connected property makes it difficult for stability analysis of the whole traffic flow mixed with CAV and Manual Driven Vehicles (MDV) which broadcast driving information to CAV under the V2V communication environment. The main reason is that stability analysis methods presented in previous studies (Mahmassani, 2016; Talebpour and Mahmassani, 2016) cannot be directly applied, because the pairs of successive vehicles cannot describe the stability condition in case of the mixed CAV flow. To deal with this, local vehicular platoons should be considered (Ge and Orosz, 2014; Qin and Wang, 2018).

The remainder of this paper is organized as follows. The local vehicular platoons and the corresponding car-following modeling are presented in Section 2. In Section 3, the methodology for stability analysis and optimization are proposed. The optimization results of CAV feedback gains are obtained. Then, passenger comfort is evaluated based on numerical simulations in Section 4. Finally, some conclusions are given in Section 5.

2. Objective and Modeling

This paper focuses on the longitudinal movement of traffic

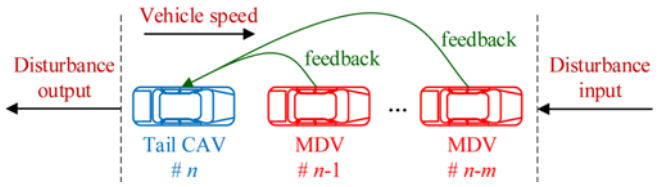

Fig. 1. The Local Vehicular Platoon with Uniform Structure

flow mixed with MDV and CAV. We assume that the MDV only needs broadcast its motion information for the CAV via V2V communication, regardless of the receiving function. This means the CAV monitors multiple vehicles ahead by using V2V communication, while the MDV only responses the immediately preceding vehicle based on the driver's reaction. These two types of vehicles are randomly distributed in the mixed traffic flow. The spatial distribution randomness requires that local vehicular platoons with uniform structure should be considered for analyzing and optimizing traffic flow stability to benefit the passenger comfort. Generally speaking, MDV is usually unstable and amplifies speed disturbances, while these disturbances are desired to be smoothed by CAV upstream. Therefore, the local vehicular platoon consists of one tail CAV and multiple MDV ahead in this paper, as shown in Fig. 1, in which the feedback means the motion information sending from the preceding MDV to the tail CAV via V2V communication. Then its optimal stability situation is determined as the objective, which can be achieved by considering the local vehicular platoon as a local system to response speed disturbances ahead. The number m of MDV ahead varies for each local vehicular platoon because of the spatial distribution randomness. Moreover, the maximum value of m is also constrained by V2V communication ranges. Hence, the whole mixed traffic flow can be theoretically divided into finite types of local vehicular platoons in terms of values of m. The objective function in this paper focuses on the stable local vehicular platoons with the uniform structure shown in Fig. 1. Because the V2V communication range may restrict the maximum number of vehicles that the tail CAV can monitor, some MDVs in the random mixed traffic flow may not be monitored and amplify the disturbances. However, the mixed traffic flow stability will be optimized based on the stable situation of each local vehicular platoon.

Car-following models are essential for the investigation of traffic flow stability. In case of MDV, many car-following models were proposed (Newell, 1961; Bando *et al*., 1995; Brackstone and McDonald 1999; Treiber *et al*., 2000; Jiang *et al*., 2001; Newell, 2002; Zhang and Kim, 2005; Chen *et al*., 2012). The Full Velocity Difference (FVD) model (Jiang *et al*., 2001) is frequently applied in the previous studies. Although the FVD model has some shortcomings, such as instability and risk of collision under some circumstances, these shortcomings are also included in the driving properties of human drivers (Tang *et al*., 2017). Therefore, the FVD model is employed here as the surrogate model for MDV. The model equation is written as follows:

$$\dot{v}_n(t) = \kappa[V(h_n(t)) - v_n(t)] + \frac{\lambda}{h_n(t)}\Delta v_n(t) \tag{1}$$

where $\dot{v}_n(t)$ is the acceleration of the vehicle n at the time t, $v_n(t)$ represents the speed, $h_n(t)$ stands for the spacing, $\Delta v_n(t)$ denotes the speed difference between two adjacent vehicles, κ and λ are sensitivity coefficients, and $V(h_n(t))$ is the optimal speed function, which is the function with respect to the spacing $h_n(t)$ and is written as:

$$V(h_n(t)) = v_0[1 - \exp(-\frac{\alpha}{v_0}(h_n(t) - s_0))] \tag{2}$$

where v_0 is the free flow speed, s_0 is the jam spacing, and α is the sensitivity parameter. Based on Wang *et al*. (2018), the calibration results of parameters in Eqs. (1) and (2) are: $v_0 = 33.0$ m/s, $\kappa = 0.629\text{s}^{-1}$, $\lambda = 4.10\text{s}^{-1}$, $\alpha = 1.26\text{s}^{-1}$, and $s_0 = 2.46$s.

The car-following control of CAV is often modeled by adding multiple feedback data into the existing model structure (Ge and Orosz, 2014; Tang *et al*., 2014; Mahmassani, 2016; Qin and Wang, 2018). These feedback data can be accelerations or speeds. Among different types of feedbacks, the feedback integrating accelerations and speeds is used for modeling CAV car-following control. It should be remarked that the methodology presented for stability optimization in the next section can be applied to various feedbacks, though one relative integrated feedback is selected here. Then the car-following model of CAV is written as follows:

$$\dot{v}_n(t) = \kappa[V(h_n(t)) - v_n(t)] + \frac{\lambda}{h_n(t)}\Delta v_n(t) + \sum_{i=1}^{m}\gamma_i f_{n,n-i}(t) \tag{3}$$

where $\gamma_i\,(0 \le \gamma_i \le 1)$ is the CAV feedback gain for the ith vehicle ahead, m is the maximum number of vehicles that the CAV can monitor, and symbol $f_{n,n-i}$ denotes the feedback data between the CAV n and the vehicle n-i ahead, which is modeled with respect to both accelerations and speeds (Li and Ioannou, 2004; Li *et al*., 2016):

$$f_{n,n-i}(t) = \frac{1}{b}(\dot{v}_{n-i}(t) - \dot{v}_n(t)) + \frac{c}{b}(v_{n-i}(t) - v_n(t)) \tag{4}$$

where b and c are sensitivity parameters, whose values are 0.27 and 0.8, respectively (Li *et al*., 2016). Eq. (4) shows that the feedback information for CAV is the sum of acceleration/speed differences between the tail CAV and all of its preceding vehicles.

3. Methodology

Because of the connected property of multiple feedbacks of CAV, existing methods in previous literatures (Mahmassani, 2016; Talebpour and Mahmassani, 2016) cannot be directly applied into the stability analysis of local vehicular platoons studied in this paper. The local vehicular platoon can be considered as a local control system. The local control system is defined as stable when disturbance input is mitigated compared with

disturbance output. Then, the stable situation means disturbances are smoothed when passing through the whole local system in the mixed traffic flow, though these disturbances may be temporarily amplified by MDV within the local system. The transfer function theory is employed to analyze and future optimize the stability of local vehicular platoons, because it has wide applications for stability analysis of control systems.

3.1 Stability Criterion

Based on the previous studies (Treiber and Kesting, 2013; Milanés and Shladover, 2014), speed disturbances are able to describe stability condition well, which are also used here for deriving stability criterion of the local vehicular platoon. It is defined as follows:

$$\tilde{v}_n(t) = v_n(t) - v \tag{5}$$

where $\tilde{v}_n(t)$ is the speed disturbance of vehicle n at the time t with respect to the equilibrium speed v. In addition to speed disturbances, spacing disturbances are also defined:

$$\tilde{h}_n(t) = h_n(t) - h \tag{6}$$

where $\tilde{h}_n(t)$ is the spacing disturbance of vehicle n at the time t with respect to the equilibrium spacing h.

In case of car-following model of MDV in Eq. (1), linearizing the model equation using Taylor expansion at the equilibrium state, it follows that:

$$\dot{v}_n(t) = -\kappa(v_n(t) - v) + \kappa V'(h(t))(h_n(t) - h) + \frac{\lambda}{h}\Delta v_n(t) \tag{7}$$

where $V'(h(t))$ is the derivative of optimal speed function in Eq. (2) to the spacing at the equilibrium state, which is calculated as follows:

$$V'(h) = \alpha \exp[-\frac{\alpha}{v_0}(h - s_0)] \tag{8}$$

As mentioned previously, h is the equilibrium spacing and has the following relation with the equilibrium speed v:

$$h = s_0 - \frac{v_0}{\alpha}\ln(1 - \frac{v}{v_0}) \tag{9}$$

Substituting Eqs. (5) and (6) into Eq. (7) to calculate the differential equation about speed and spacing disturbances:

$$\dot{\tilde{v}}_n(t) = -\kappa\tilde{v}_n(t) + \kappa V'(h)\tilde{h}_n(t) + \frac{\lambda}{h}\Delta\tilde{v}_n(t) \tag{10}$$

Taking the Laplace transform of Eq. (10) with zero initial conditions to calculate the transfer function $G_1(s)$ of speed disturbances passing a MDV:

$$G_1(s) = \frac{\kappa V'(h) + \frac{\lambda}{h}s}{s^2 + (\frac{\lambda}{h} + \kappa)s + \kappa V'(h)} \tag{11}$$

where s denotes the Laplace domain.

The transfer function of speed disturbances passing a CAV should be also calculated to obtain the transfer function of speed disturbances passing through the whole local vehicular platoon.

Substituting Eqs. (5) and (6) into Eq. (4) and then substituting the result equation into Eq. (3) to calculate the differential equation about speed and spacing disturbances in the case of the CAV car-following model:

$$\dot{\tilde{v}}_n(t) = -\kappa\tilde{v}_n(t) + \kappa V'(h)\tilde{h}_n(t) + \frac{\lambda}{h}\Delta\tilde{v}_n(t) + \frac{1}{b}\sum_{i=1}^{m}\gamma_i[\dot{\tilde{v}}_{n-i}(t) - \dot{\tilde{v}}_n(t) + c(\tilde{v}_{n-i}(t) - \tilde{v}_n(t))] \tag{12}$$

Taking the Laplace transform of Eq. (12) with zero initial conditions to calculate the transfer function $G_2(s)$ of speed disturbances passing a CAV:

$$G_2(s) = \frac{\kappa V'(h) + \frac{\lambda}{h}s + [(s^2 + cs)/b]\sum_{i=1}^{m}\gamma_i(\frac{\kappa V'(h) + \frac{\lambda}{h}s}{s^2 + (\frac{\lambda}{h} + \kappa)s + \kappa V'(h)})^{(i-1)}}{s^2 + (\frac{\lambda}{h} + \kappa)s + \kappa V'(h) + [(s^2 + cs)/b]\sum_{i=1}^{m}\gamma_i} \tag{13}$$

Based on the transfer function theory, the transfer function $G(s)$ of speed disturbances passing through the whole local vehicular platoon is calculated as follows:

$$G(s) = G_2(s)[G_1(s)]^m = \left[\frac{\kappa V'(h) + \frac{\lambda}{h}s + [(s^2 + cs)/b]\sum_{i=1}^{m}\gamma_i(\frac{\kappa V'(h) + \frac{\lambda}{h}s}{s^2 + (\frac{\lambda}{h} + \kappa)s + \kappa V'(h)})^{(i-1)}}{s^2 + (\frac{\lambda}{h} + \kappa)s + \kappa V'(h) + [(s^2 + cs)/b]\sum_{i=1}^{m}\gamma_i}\right]\left[\frac{\kappa V'(h) + \frac{\lambda}{h}s}{s^2 + (\frac{\lambda}{h} + \kappa)s + \kappa V'(h)}\right]^m \tag{14}$$

Let $s = \mathrm{j}\Omega$ ($\Omega \geq 0$) to convert Eq. (14) from Laplace domain to frequency domain. Then, the local vehicular platoon will be stable if the following stability criterion is satisfied:

$$|G(\mathrm{j}\Omega)| = \left|\frac{\kappa V'(h) + \mathrm{j}\frac{\lambda}{h}\Omega + [(-\Omega^2 + \mathrm{j}c\Omega)/b]\sum_{i=1}^{m}\gamma_i(\frac{\kappa V'(h) + \mathrm{j}\frac{\lambda}{h}\Omega}{\kappa V'(h) - \Omega^2 + \mathrm{j}(\frac{\lambda}{h} + \kappa)\Omega})^{(i-1)}}{\kappa V'(h) - \Omega^2 + \mathrm{j}(\frac{\lambda}{h} + \kappa)\Omega + [(-\Omega^2 + \mathrm{j}c\Omega)/b]\sum_{i=1}^{m}\gamma_i}\right| \cdot \left|\frac{\kappa V'(h) + \mathrm{j}\frac{\lambda}{h}\Omega}{\kappa V'(h) - \Omega^2 + \mathrm{j}(\frac{\lambda}{h} + \kappa)\Omega}\right|^m < 1 \tag{15}$$

where jΩ stands for the frequency domain, and |•| denotes the amplitude of transfer function in the frequency domain.

According to the stability criterion derived in Eq. (15), the stability situation is determined by the CAV feedback gain γ_i and the equilibrium speed v that determines the equilibrium spacing h. This property can be used to calculate the stability chart with respect to equilibrium speeds and CAV feedback gains. Then, the CAV feedback gains can be controlled to achieve the optimal stability situation for local vehicular platoons with each value of m.

3.2 Stability Optimization Results

As mentioned previously, the maximum value of the feedback number m of CAV is limited by V2V communication ranges. At the current stage, the V2V communication range is about 200m to 300 m, based on which the maximum value of m is selected as 3 as an example in the previous studies (Ge and Orosz, 2014; Qin and Wang, 2018). It should be mentioned that the stability criterion presented in Eq. (15) can be applied for any value of m.

3.2.1 m = 1

In this case, there is one CAV feedback gain γ_1. Based on the stability criterion derived in Eq. (15), the stability chart of the local vehicular platoon with respect to the equilibrium speed v and the CAV feedback gain γ_1 is calculated, as shown in Fig. 2. The blue region stands for stabile situation, while the red region denotes unstable situation. From the perspective of optimal stability of the local vehicular platoon, whether the local vehicular platoon can be always stable at any equilibrium speed is concerned. This concern can be achieved if the CAV feedback gain γ_1 is controlled to be the range of [0.445, 1], according to the calculation result in Fig. 2.

3.2.2 m = 2

This case has two CAV feedback gains, namely γ_1 and γ_2. Following the stability criterion in Eq. (15), the stability condition of the local vehicular platoon can be also calculated. Note that the

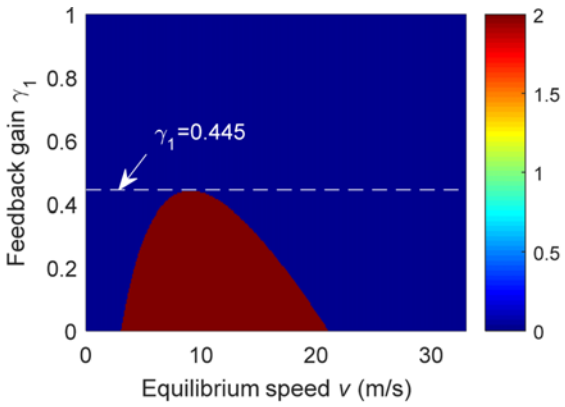

Fig. 2. Stability Chart for the Case of m = 1

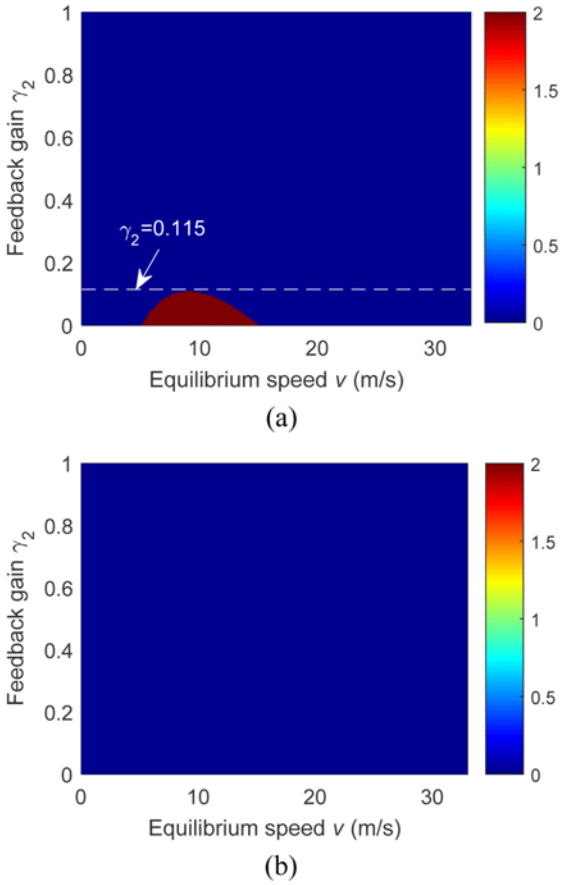

Fig. 3. Stability Chart for the Case of m = 2: (a) γ_1 = 0.445, (b) γ_1 = 1

optimal value range of γ_1 has been obtained in Fig. 2. Then the values of γ_1 are substituted into calculations for the stability chart of the local vehicular platoon with respect to the equilibrium speed v and the CAV feedback gain γ_2. It is found that the larger value of γ_1 has better stability situation for controlling γ_2, as shown in Fig. 3. When γ_1 increases to 1, γ_2 needs not be controlled, because the local vehicular platoon maintains stable under any values of both γ_2 and v. However, the sufficient condition for optimal stability situation of the local vehicular platoon should be considered in the implement of controlling γ_2. Therefore, the optimal control result of the gain γ_2 is obtained: [0.115, 1], when γ_1 is equal to be 0.445.

3.2.3 m = 3

In this case, there are three CAV feedback gains: γ_1, γ_2, and γ_3. The stability chart of the local vehicular platoon with respect to the equilibrium speed v and the CAV feedback gain γ_3 is calculated in this case, based on the optimal control ranges of γ_1 and γ_2. It is also found that the sufficient optimal control result of γ_3 should be determined when γ_1 and γ_2 are both equal to the lower bounds of their optimal control ranges, respectively. The calculation result is shown in Fig. 4, in which γ_1 is equal to 0.445 and γ_2 is 0.115. Then the optimal control result of the gain γ_3 is the range of [0.075, 1].

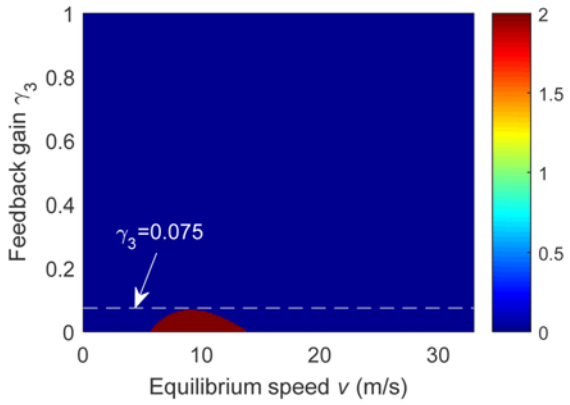

Fig. 4. Stability Chart for the Case of m = 3

4. Evaluating Passenger Comfort

4.1 Evaluating Indicator

The evaluating indicator called Comfort Index (CI) (Paddan and Griffin, 2002) is employed to evaluate passenger comfort of traffic flow based on numerical simulations. The CI is described by the International Organization for Standardization (ISO) 2631-1. As noted before, the longitudinal movement of vehicles is concerned, while the lane-change behavior is not considered in this paper because lane-change strategies for CAV are quite complex and still under studied. Therefore, under car-following models, the CI equation can be simplified as follows:

$$CI=[\frac{1}{N}\sum_{i=0}^{N}a_i^2]^{1/2} \tag{16}$$

where a_i is the i^{th} acceleration obtained based on simulations, N is the total number of all vehicles' accelerations. Moreover, the smaller value of CI indicates more comfortable feelings in the traffic flow.

According to Eq. (16), the CI is determined by acceleration dynamics. Because speed dynamics may also affect passenger comfort, the variance of speeds in simulations is also evaluated as another indicator. Based on car-following simulations, the speeds and accelerations (a_i in Eq. (16)) of all vehicles over all simulation time can be obtained, which are known as the microcosmic simulation trajectory data. Then the CI can be calculated by substituting each vehicle's acceleration at each simulation time into Eq. (16), while each vehicle's speeds over its simulation time are used to calculate the variance of speeds of all vehicles. It should be mentioned that the CI in Eq. (16) describes the average comfort of all vehicles over the simulation time from the perspective of the entire traffic flow (Paddan and Griffin, 2002).

4.2 Simulations and Results

Numerical simulations are important ways to evaluate CAV impacts on traffic flow (Treiber and Kesting, 2013; Milanés and Shladover, 2014; Mahmassani, 2016; Talebpour and Mahmassani, 2016). The highway with an on-ramp is a typical bottleneck, in which simulations are conducted here to evaluate the passenger comfort using car-following models and the stability optimization results of local vehicular platoons. The simulation segment is a hypothetical one-lane highway with an on-ramp located in the middle of the segment (Mahmassani, 2016; Talebpour and Mahmassani, 2016), in which the length of the simulation segment is about 6.5 km. The initial speeds of vehicles are randomly determined from 25 m/s to 30 m/s. The main-line flow is set to 400 veh/h, 600 veh/h, 1,100 veh/h, 1,400 veh/h, 1,800 veh/h and 2,200 veh/h respectively, while the ramp flow is 360 veh/h. All the parameters needed for simulations are set according to the recent studies (Mahmassani, 2016; Talebpour and Mahmassani, 2016). Numerical simulations are implemented in Matlab, a computational software package, by using car-following models of CAV and MDV. In simulations, vehicles arrive into the simulation segment based on the flow set. The types of arrival vehicles are randomly determined by the CAV penetration rate that is previously set in the Matlab program for each simulation. Therefore, the vehicle orders are also random in the mixed vehicular flow. The total simulation time is one hour, the simulation time step is 0.1s. The desired vehicle speed is set as 33.0 m/s, the maximum acceleration is set as 4 m/s^2, and the emergency deceleration is set as −6 m/s^2 (Ni *et al*., 2015). For each time step, the vehicles update their positions, speeds, and accelerations, one by one from downstream to upstream, based on the corresponding car-following model formula. Then the simulation trajectory data of all vehicles, namely positions, speeds, and accelerations, over all simulation time are obtained.

Note that the stability optimization results of local vehicular platoons in the above section gives the optimal value ranges of CAV feedback gains. Without loss of generality, the intermediate values of the optimal results of each CAV feedback gain were used in simulations. This means the maximum number of vehicles that one CAV can monitor is three. Because of the randomness of vehicle orders, one CAV randomly monitors one, two, or three vehicles ahead in simulations, based on the uniform structure shown in Fig. 1. Additionally, the tail CAV can also monitor CAV ahead when successive CAV appear and the corresponding stability optimization results were used. Because the main-line flow is usually disturbed by the ramp flow, what are mainly concerned should be the main-line comfort situations. This means only main-line vehicles are considered to calculate the simulation results (Mahmassani, 2016; Talebpour and Mahmassani, 2016). Meanwhile, the type of the vehicle that is entering the main-line from the ramp is randomly determined based on the CAV penetration rate previously set in the simulation. Moreover, the lane-changing model applied here is the MOBIL (minimizing overall braking induced by lane change) proposed by Kesting *et al*. (2007). Based on simulations, the values of CI and the variance of speeds were calculated, in which the sampling interval for evaluating indicators was 1 s. Taking into consideration the randomness of vehicles' relative space positions, every simulation was repeated for five times for each CAV penetration rate. Then the average value was obtained as the result of the

Table 1. Percentage Reductions of Evaluating Indicators Compared with 0% CAV under High Flows

CAV penetration rates	Average reducing (%)			
	Main-line flow: 1,800veh/h		Main-line flow: 2,200veh/h	
	Values of CI	Variance of speeds	Values of CI	Variance of speeds
0%	1.8426 m/s^2	18.3695 (m/s)^2	2.2623 m/s^2	20.1163 (m/s)^2
10%	7.3973	7.7864	10.4683	7.5004
20%	13.4427	13.5629	21.7142	13.6751
30%	17.2249	16.8481	29.5334	18.6673
40%	19.3666	18.8061	33.6524	22.0462
50%	22.8982	21.7611	35.6008	23.3974
60%	23.7336	24.0732	38.1131	25.1538
70%	25.5487	27.0468	39.5402	26.5248
80%	26.3841	28.3748	40.6683	28.7203
90%	26.6500	29.7113	40.8050	29.9877
100%	26.6576	31.6481	40.9417	31.3898

Table 2. Percentage Reductions of Evaluating Indicators Compared with 0% CAV under Medium Flows

CAV penetration rates	Average reducing (%)			
	Main-line flow: 1,100veh/h		Main-line flow: 1,400veh/h	
	Values of CI	Variance of speeds	Values of CI	Variance of speeds
0%	1.3302 m/s^2	12.1977 (m/s)^2	1.4686 m/s^2	13.9829 (m/s)^2
10%	1.8317	2.5295	2.6237	2.3529
20%	3.1459	3.5622	5.4428	5.5281
30%	3.7178	5.3072	5.6157	7.0144
40%	4.2898	7.6536	8.9911	9.1017
50%	4.7256	8.8415	9.7053	10.7692
60%	5.0933	11.1043	10.6676	13.4206
70%	5.1001	11.7064	10.8630	15.2357
80%	5.1069	13.9606	11.1487	17.1844
90%	5.1478	15.6863	11.5622	18.6912
100%	5.7470	16.9149	11.5847	20.3391

Table 3. Percentage Reductions of Evaluating Indicators Compared with 0% CAV under Low Flows

CAV penetration rates	Average reducing (%)			
	Main-line flow: 400veh/h		Main-line flow: 600veh/h	
	Values of CI	Variance of speeds	Values of CI	Variance of speeds
0%	1.1702 m/s^2	10.6127 (m/s)^2	1.3167 m/s^2	11.7770 (m/s)^2
10%	0.2388	0.4686	1.3092	0.6876
20%	0.5590	0.5437	1.6147	1.2673
30%	0.6133	1.7572	1.6535	2.4916
40%	0.6675	2.8753	1.9735	2.8199
50%	0.8846	3.6240	2.0172	3.2412
60%	0.9443	4.6791	2.1481	4.3120
70%	1.1343	5.0415	2.2596	5.1090
80%	1.2428	5.3489	2.7057	6.1880
90%	1.6987	6.0236	3.5058	7.1744
100%	1.7041	7.1094	3.7046	8.5517

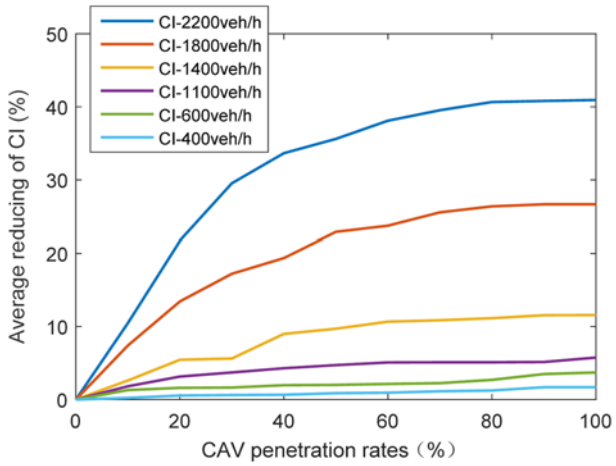

Fig. 5. Average Percentage Reductions of CI with the Increase of the CAV Penetration Rate

evaluating indicator. The simulation results for 0% CAV traffic flow were considered to be the benchmark, compared with which percentage reductions of evaluating indicators were obtained for different CAV penetration rates, as shown in Table 1, Table 2, and Table 3, respectively. Table 1 shows the simulation results under the high flow scenarios, in which the main-line flow is 1,800 veh/h and 2,200 veh/h. Moreover, Table 2 shows the simulation results of the medium flows of 1,100 veh/h and 1400 veh/h, while the low flow scenarios of 400 veh/h and 600 veh/h are shown in Table 3. In the Tables, the values of the first row are the average simulation values of the CI and the variance of speeds for the baseline 0% CAV penetration scenario. The values of the other rows are the percentage reductions for the other CAV penetration rates, compared with 0% CAV penetration scenario.

According to the Tables 1, 2, and 3, values of CI and the variance of speeds both decrease with the increase of CAV penetration rates, under these cases of the main-line flows. This indicates that passenger comfort situation is gradually improved because of the increase of CAV penetration rates. When CAV penetration rates reach to 100%, the passenger comfort described by CI can be improved by 26.6576–40.9417% for the high flow scenarios, 5.7470–11.5847% for the medium flow scenarios, and 1.7041–3.7046% for the low flow scenarios, respectively. Meanwhile, the variance of speeds can be decreased by 31.3898–31.6481% for the high flow scenarios, 16.9149–20.3391% for the medium flow scenarios, and 7.1094–8.5517% for the low flow scenarios, respectively.

For better visualization, the figures indicating the improvements are calculated based on these simulation results, as shown in Figs. 5 and 6. Fig. 5 shows the average percentage reductions of CI with the increase of the CAV penetration rate, while the average percentage reductions of the speed variance are described in Fig. 6 under different main-line flow scenarios. It can be seen that the improvements of the passenger comfort increase with the increase of the main-line flow. Because the high flow scenarios are likely to result in congested traffic situations, it indicates that

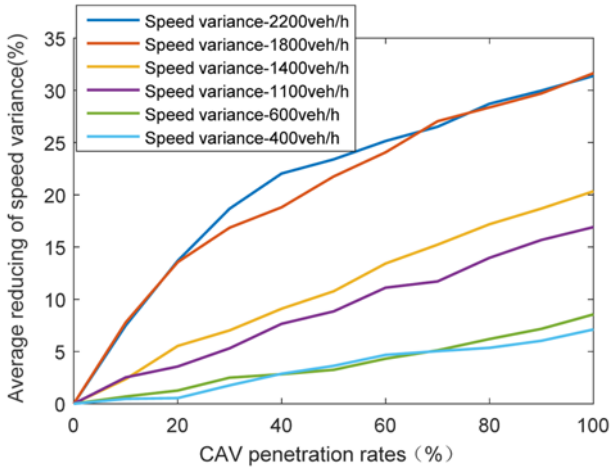

Fig. 6. Average Percentage Reductions of Speed Variance with the Increase of the CAV Penetration Rate

the proposed method in this paper is more helpful to enhance passenger comfort of the congestion situations. Besides, it should be noted that the CI is calculated based on the vehicle accelerations in simulations, while the speed variance is calculated according to the vehicle speeds. Then the simulation values of CI are small, while those of the speed variance are large. In the case of small simulation values, smaller difference is apt to result in larger percentage reductions. Therefore, the speed variances of the two similar flow scenarios are of the same level, while CI may be quite different at the same penetration rate. The reason for this difference is essentially determined by the relationship between simulation values and the corresponding benchmark values. The CI and speed variance are two different evaluating indicators with different units, though they are both used to reflect the passenger comfort in this paper. Therefore, this difference in Figs. 5 and 6 may be naturally reasonable. What this paper mainly concern is that the proposed method is helpful for improving passenger comfort, which focuses on the qualitative trend. Both Figs. 5 and 6 depict the same qualitative trend of the CI and the speed variance, while the quantitative reductions of speed variance in Fig. 6 are apt to be similar for the high flow scenarios and low flow scenarios under some values of CAV penetration rates.

5. Discussions

5.1 Comparison with the Previous Controller

In order to further show the improvement of the proposed method in this paper, we perform simulations by using another intelligent controller for the comparison. The controller used for the comparison is the enhanced Intelligent Driver Model (IDM) (Kesting *et al.*, 2010). In this paper, the proposed method for reducing passenger comfort focuses on controlling the individual CAV in the mixed traffic flow. Then in the case of the enhance IDM, the individual CAV is controlled by the enhance IDM. The enhanced IDM was proposed by Keating *et al*. (2010) based on the original IDM (Treiber *et al*., 2000). The original IDM can be written as follows:

$$\dot{v}_{IDM} = a[1-(\frac{v}{v_0})^4 - (\frac{s_0 + vT + \frac{v\Delta v}{2\sqrt{ab}}}{s})^2] \tag{17}$$

where $\dot{v}_{IDM}$ is the acceleration by the original IDM, a is the maximum acceleration, v is the following vehicle's speed, v_0 is the free flow speed, s_0 is the minimum safety distance, T is the safety headway, Δv is the speed difference, b is the comfort deceleration, and s is the distance gap to the leading vehicle.

Based on Keating *et al*. (2010), Constant-Acceleration Heuristic (CAH) should be considered. The CAH assumption is given by:

$$\dot{v}_{CAH} = \begin{cases} \dfrac{v^2\tilde{a}_l}{v_l^2 - 2s\tilde{a}_l} & if\ v_l(v-v_l) \le -2s\tilde{a}_l \\ \tilde{a}_l - \dfrac{(v-v_l)^2\Theta(v-v_l)}{2s} & otherwise \end{cases} \tag{18}$$

where $\dot{v}_{CAH}$ is the acceleration based on the CAH, $\tilde{a}_l = \min\{\dot{v}_l, a\}$ is the effective acceleration, in which $\dot{v}_l$ is the acceleration of the leading vehicle and a is the maximum acceleration parameter of IDM. v_l is speed of the leading vehicle, v and s have the same meanings with those in Eq. (17). Besides, Θ stands for the Heaviside step function, which means $\Theta(x)=1$ if $x \ge 0$, and zero, otherwise.

Based on Eqs. (17) and (18), the enhanced IDM is presented as follows:

$$\dot{v}_{Enhanced\ IDM} = \begin{cases} \dot{v}_{IDM} & \dot{v}_{IDM} \ge \dot{v}_{CAH} \\ (1-c)\dot{v}_{IDM} + c[\dot{v}_{CAH} + b\tanh(\dfrac{\dot{v}_{IDM} - \dot{v}_{CAH}}{b})] & otherwise \end{cases} \tag{19}$$

where $\dot{v}_{Enhanced\ IDM}$ denotes the acceleration of the enhanced IDM, and c is the coolness factor. According to Keating *et al*. (2010), the model parameters are set as: $v_0 = 33.0$ m/s, $T = 1.5$s, $s_0 = 2.0$ m, $a = 1.4$ m/s^2, $b = 2.0$ m/s^2, and $c = 0.99$.

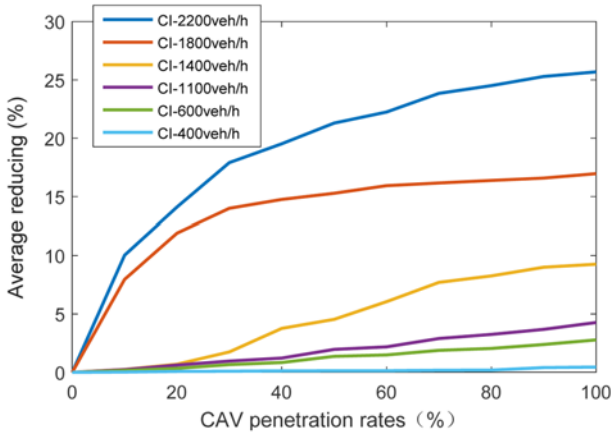

Fig. 7. Average Percentage Reductions of CI with the Increase of the CAV Penetration Rate in the Case of the Enhanced IDM

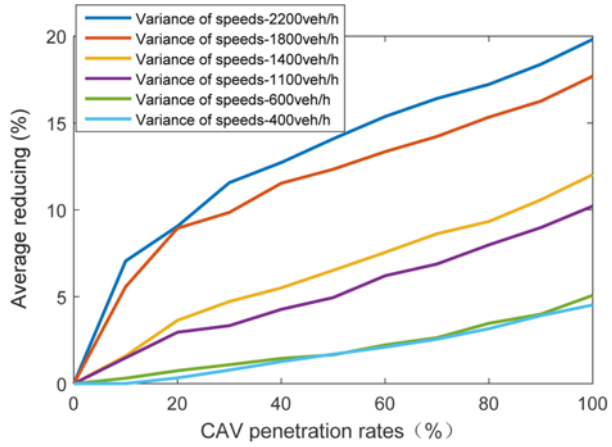

Fig. 8. Average Percentage Reductions of Speed Variance with the Increase of the CAV Penetration Rate in the Case of the Enhanced IDM

Simulation designs are considered the same with those in Section 4, based on which simulation results of the enhance IDM are obtained. For better visualization, the figures indicating the improvements are calculated based on these simulation results of the enhance IDM, as shown in Figs. 7 and 8. Fig. 7 shows the average percentage reductions of CI with the increase of the CAV penetration rate by the enhance IDM, while the average percentage reductions of the speed variance are described in Fig. 8 under different main-line flow scenarios. In Fig. 7, the controller of the enhanced IDM can reduce CI by 25.6885%, 16.9574%, 9.2576%, 4.2675%, 2.7725%, and 0.4362% under the six flows, respectively, if the CAV penetration rate increases to 1. Meanwhile, Fig. 8 shows that the enhanced IDM can reduce speed variance by 19.8162%, 17.6907%, 12.0322%, 10.2123%, 5.0803%, and 4.5285%, respectively, for different traffic scenarios with 100% CAV flow. By comparing Figs. 5 through 8, it indicates that the proposed method in this paper has more benefits than the enhanced IDM in improving passenger comfort.

5.2 Collision Risks Evaluation

In this paper, the FVD model is used as the basic car-following model. Because the FVD model has the shortcoming of collision risks (Tang *et al.*, 2017), this section considers the collision risk as one of passenger comfort indicators and evaluate the impacts of the proposed method in this paper on collision risks.

According to previous studies (Meng and Weng, 2011; Vogel 2003; Weng *et al.*, 2015), the Deceleration Rate to Avoid the Crash (DRAC) was widely used to evaluate collision risks. Then we also used the DRAC as the collision indicator here, which is calculated as follows:

$$DRAC_n^{n-1} = \begin{cases} \dfrac{(v_n - v_{n-1})^2}{d}, & \forall v_n > v_{n-1} \\ 0, & \forall v_n \le v_{n-1} \end{cases} \tag{20}$$

where v_n is the following vehicle's speed, while v_{n-1} is the leading vehicle's speed, and d denotes the spacing distance between the two adjacent vehicles. Eq. (20) shows that there are risks of collisions if and only if the following vehicle has larger speed than the leading vehicle. Therefore, $DRAC_n^{n-1}$ denotes the deceleration rate of the vehicle n to avoid the crash with the vehicle n-1. In the case of car-following behaviors, vehicle n also has probability being collided by the lag vehicle $n+1$. Therefore, the probability of crash risk for vehicle n at the time t, labeled by $p_{n,t}$, is calculated as follows (Meng and Weng, 2011):

$$p_{n,t} = p(DRAC_{n,t}^{n-1} > MADR_{n,t}) + p(DRAC_{n+1,t}^{n} > MADR_{n+1,t}) \tag{21}$$

where $p(DRAC_{n,t}^{n-1} > MADR_{n,t})$ is the crash risk between vehicle n and n-1 at time t, while $DRAC_{n+1,t}^{n} > MADR_{n+1,t}$ denotes the crash risk between vehicle n and $n+1$ at time t. The MADR denotes the maximum available deceleration rate, which is usually considered to follow a truncated normal distribution (Meng and Weng, 2011): The mean is 8.45 m/s^2, the standard deviation is 1.40 m/s^2, the upper limit is 12.68 m/s^2, and the lower limit is 1.23 m/s^2.

According to Eq. (21), the average crash risk of total vehicles over the whole simulation period can be calculated as follows:

$$R = \frac{\sum_{n=1}^{N}\sum_{t=0}^{T} p_{n,t}\Delta T}{N} \tag{22}$$

where R is the collision risk, N is the number of vehicles calculated for collision risks, T is the simulation time, and Δt is the time interval which is equal to be the simulation time step.

Based on the simulations under different CAV penetration rates and flow scenarios, we calculate the corresponding collision risks. The collision risk for the 0% CAV penetration rate is also considered as the benchmark. Then the reductions of the collision risks with the increase of the CAV penetration rate are calculated, as shown in Fig. 9. From the qualitative perspective, the collision risks decrease with the increase of CAV penetration rates for different

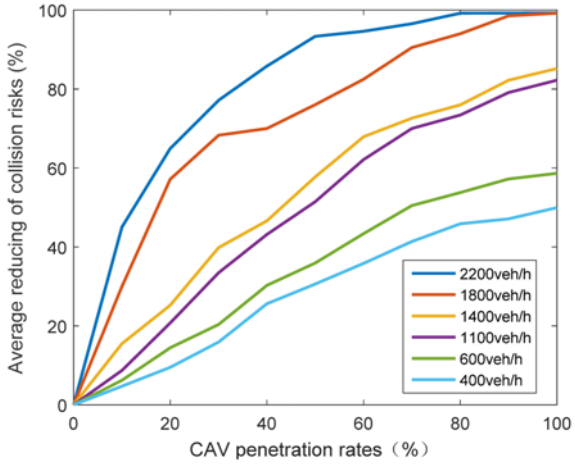

Fig. 9. Average Percentage Reductions of Collision Risks with the Increase of the CAV Penetration Rate

traffic scenarios. This indicates that the proposed method in this paper is also helpful for reducing collision risks.

6. Conclusions

Although some recent review studies (Elbanhawi *et al*., 2015; Milakis *et al*., 2017; Yang *et al*., 2017) all point out the critical knowledge gap about CAV impact on passenger comfort, little research have been conducted. This paper presents an effort to fill this research gap from the perspective of traffic flow stability. The existing methods in previous literatures (Mahmassani, 2016; Talebpour and Mahmassani, 2016) cannot be easily employed for stability analysis of the mixed CAV flow, in which CAV receives multiple feedbacks from vehicles ahead via V2V communications. This paper considers local vehicular platoons with uniform structure as local control systems, then presents the stability analysis and optimization method. The presented methodology can calculate the stability chart of the local vehicular platoon with respect to equilibrium speeds and CAV feedback gains. Based on the stability chart, CAV feedback gains can be controlled for optimal stability situation, where the local vehicular platoon keep stable at any equilibrium speeds. Taking the V2V communication range into consideration, the maximum number of CAV feedback is selected to be 3 as an example. Calculations of stability charts show that the optimal control ranges of the first, second, and third gains of CAV are [0.445, 1], [0.115, 1], and [0.075, 1], respectively.

Importantly, this paper focuses on improving passenger comfort by enhancing stability of the traffic flow mixed with CAV and MDV. The CAV impact on passenger comfort under the optimal stability of local vehicular platoons is evaluated using numerical simulations. It indicates that the passenger comfort described by ISO 2631-1 can be improved by 26.6576-40.9417% under high main-line flow conditions of the highway described in the studies (Mahmassani, 2016; Talebpour and Mahmassani, 2016). At the same time, the variance of speeds can be decreased by 31.3898-31.6481% for the high flow scenarios, which is also related with the enhancement of the passenger comfort, when the 100% CAV flow is compared with that of 0% CAV. It indicates that the stable traffic flow is more helpful for improving the passenger comfort in the traffic congestion situations.

Theoretical analysis and numerical simulations cannot fully describe passenger comfort for CAV driving, though it gives good CAV control strategies on improving passenger comfort. People's real experience will be the true feeling of the passenger comfort. Hence, real CAV experiments are important to accurately evaluate the impact of CAV on passenger comfort. Because implementations of these control strategies suggested by the theoretical analysis in production vehicles are often costly, driving simulators will be very helpful to deal with this before real vehicle tests and is remained for further study.

Acknowledgements

This work was supported by the National Natural Science Foundation of China (51478113); the National Key R&D Program in China (2016YFB0100906); the Fundamental Research Funds for the Central Universities and the Postgraduate Research & Practice Innovation Program of Jiangsu Province (KYCX17_0146); and the Scientific Research Foundation of Graduate School of Southeast University (YBJJ1792).

References

Bando, M., Hasebe, K., Nakayama, A., Shibata, A., and Sugiyama, Y. (1995). "Dynamical model of traffic congestion and numerical simulation." *Physical Review E*, Vol. 51, No. 2, pp. 1035-1042, DOI: 10.1103/PhysRevE.51.1035.

Bellem, H., Schönenberg, T., Krems, J. F., and Schrauf, M. (2016). "Objective metrics of comfort: developing a driving style for highly automated vehicles." *Transportation Research Part F: Traffic Psychology and Behaviour*, Vol. 41, pp. 45-54, DOI: 10.1016/j.trf.2016.05.005.

Brackstone, M. and McDonald, M. (1999). "Car-following: a historical review." *Transportation Research Part F: Traffic Psychology and Behaviour*, Vol. 2, No. 4, pp. 181-196, DOI: 10.1016/S1369-8478(00)00005-X.

Chen, D., Laval, J., Zheng, Z., and Ahn, S. (2012). "A behavioral car-following model that captures traffic oscillations." *Transportation Research Part B: Methodological*, Vol. 46, No. 6, pp. 744-761, DOI: 10.1016/j.trb.2012.01.009.

Dang, R., Wang, J., Li, S. E., and Li, K. (2015). "Coordinated adaptive cruise control system with lane-change assistance." *IEEE Transactions on Intelligent Transportation Systems*, Vol. 16, No. 5, pp. 2373-2383, DOI: 10.1109/TITS.2015.2389527.

Elbanhawi, M., Simic, M., and Jazar, R. (2015). "In the passenger seat: investigating ride comfort measures in autonomous cars." *IEEE Intelligent Transportation Systems Magazine*, Vol. 7, No. 3, pp. 4-17, DOI: 10.1109/MITS.2015.2405571.

Fleiter, J. J., Lennon, A., and Watson, B. (2010). "How do other people influence your driving speed? Exploring the 'who'and the 'how'of social influences on speeding from a qualitative perspective." *Transportation Research Part F: Traffic Psychology and Behaviour*, Vol. 13, No. 1, pp. 49-62, DOI: 10.1016/j.trf.2009.10.002.

Ge, J. I. and Orosz, G. (2014). "Dynamics of connected vehicle systems with delayed acceleration feedback." *Transportation Research Part C: Emerging Technologies*, Vol. 46, pp. 46-64, DOI: 10.1016/j.trc.2014.04.014.

Glaser, S., Vanholme, B., Mammar, S., Gruyer, D., and Nouveliere, L. (2010). "Maneuver-based trajectory planning for highly autonomous vehicles on real road with traffic and driver interaction." *IEEE Transactions on Intelligent Transportation Systems*, Vol. 11, No. 3, pp. 589-606, DOI: 10.1109/TITS.2010.2046037.

Hoogendoorn, R., van Arem, B., and Hoogendoorn, S. (2014). "Automated driving, traffic flow efficiency, and human factors: Literature review." *Transportation Research Record: Journal of the Transportation Research Board*, Vol. 2422, pp. 113-120, DOI: 10.3141/2422-13.

Jayachandran, R. and Krishnapillai, S. (2013). "Modeling and optimization of passive and semi-active suspension systems for passenger cars to improve ride comfort and isolate engine vibration." *Journal of Vibration and Control*, Vol. 19, No. 10, pp. 1471-1479, DOI: 10.1177/1077546312445199.

Jia, D. and Ngoduy, D. (2016). "Enhanced cooperative car-following traffic model with the combination of V2V and V2I communication." *Transportation Research Part B: Methodological*, Vol. 90, pp. 172-

191, DOI: 10.1016/j.trb.2016.03.008.

Jiang, R., Wu, Q., and Zhu, Z. (2001). "Full velocity difference model for a car-following theory." *Physical Review E*, Vol. 64, No. 1, pp. 017101, DOI: 10.1103/PhysRevE.64.017101.

Kesting, A. and Treiber, M. (2013). *Traffic flow dynamics: Data, models and simulation*, Springer-Verlag, New York, USA.

Kesting, A., Treiber, M., and Helbing, D. (2007). "General lane-changing model MOBIL for car-following models." *Transportation Research Record*, Vol. 1999, No. 1, pp. 86-94, DOI: 10.3141/1999-10.

Kesting, A., Treiber, M., and Helbing, D. (2010). "Enhanced intelligent driver model to access the impact of driving strategies on traffic capacity." *Philosophical Transactions of the Royal Society of London A: Mathematical, Physical and Engineering Sciences*, Vol. 368, No. 1928, pp. 4585-4605, DOI: 10.1098/rsta.2010.0084.

Lefèvre, S., Carvalho, A., and Borrelli, F. (2016). "A learning-based framework for velocity control in autonomous driving." *IEEE Transactions on Automation Science and Engineering*, Vol. 13, No. 1, pp. 32-42, DOI: 10.1109/TASE.2015.2498192.

Li, K. and P. Ioannou. (2004). "Modeling of traffic flow of automated vehicles." *IEEE Transactions on Intelligent Transportation Systems*, Vol. 5, No. 2, pp. 99-113, DOI: 10.1109/TITS.2004.828170.

Li, S., Li, K., Rajamani, R., and Wang, J. (2011). "Model predictive multi-objective vehicular adaptive cruise control." *IEEE Transactions on Control Systems Technology*, Vol. 19, No. 3, pp. 556-566, DOI: 10.1109/TCST.2010.2049203.

Li, Y., Zhang, L., Peeta, S., He, X., Zheng, T., and Li, Y. (2016). "A car-following model considering the effect of electronic throttle opening angle under connected environment." *Nonlinear Dynamics*, Vol. 85, No, 4, pp. 2115-2125, DOI: 10.1007/s11071-016-2817-y.

Lin, C. F., Juang, J. C., and Li, K. R. (2014). "Active collision avoidance system for steering control of autonomous vehicles." *IET Intelligent Transport Systems*, Vol. 8, No. 6, pp. 550-557, DOI: 10.1049/iet-its.2013.0056.

Luo, Y., Chen, T., Zhang, S., and Li, K. (2015). "Intelligent hybrid electric vehicle ACC with coordinated control of tracking ability, fuel economy, and ride comfort." *IEEE Transactions on Intelligent Transportation Systems*, Vol. 16, No. 4, pp. 2303-2308, DOI: 10.1109/TITS.2014.2387356.

Mahmassani, H. S. (2016). "50th anniversary invited article—autonomous vehicles and connected vehicle systems: Flow and operations considerations." *Transportation Science*, Vol. 50, No. 4, pp. 1140-1162, DOI: 10.1287/trsc.2016.0712.

Meng, Q. and Weng, J. (2011). "Evaluation of rear-end crash risk at work zone using work zone traffic data." *Accident Analysis & Prevention*, Vol. 43, No. 4, pp. 1291-1300, DOI: 10.1016/j.aap.2011.01.011.

Milakis, D., Van Arem, B., and Van Wee, B. (2017). "Policy and society related implications of automated driving: A review of literature and directions for future research." *Journal of Intelligent Transportation Systems*, Vol. 21, No, 4, pp. 324-348, DOI: 10.1080/15472450.2017.1291351.

Milanés, V. and Shladover, S. E. (2014). "Modeling cooperative and autonomous adaptive cruise control dynamic responses using experimental data." *Transportation Research Part C: Emerging Technologies*, Vol. 48, pp. 285-300, DOI: 10.1016/j.trc.2014.09.001.

Moon, S., Moon, I., and Yi, K. (2009). "Design, tuning, and evaluation of a full-range adaptive cruise control system with collision avoidance." *Control Engineering Practice*, Vol. 17, No. 4, pp. 442-455, DOI: 10.1016/j.conengprac.2008.09.006.

Newell, G. F. (1961). "Nonlinear effects in the dynamics of car following." *Operations Research*, Vol. 9, No. 2, pp. 209-229, DOI: 10.1287/opre.9.2.209.

Newell, G. F. (2002). "A simplified car-following theory: a lower order model." *Transportation Research Part B: Methodological*, Vol. 36, No. 3, pp. 195-205, DOI: 10.1016/S0191-2615(00)00044-8.

Ngoduy, D. (2013). "Instability of cooperative adaptive cruise control traffic flow: A macroscopic approach." *Communications in Nonlinear Science and Numerical Simulation*, Vol. 18, No. 10, pp. 2838-2851, DOI: 10.1016/j.cnsns.2013.02.007.

Ni, D., Leonard, J. D., Jia, C., and Wang, J. (2015). "Vehicle longitudinal control and traffic stream modeling." *Transportation Science*, Vol. 50, No. 3, pp. 1016-1031, DOI: 10.1287/trsc.2015.0614.

Paddan, G. S. and Griffin, M. J. (2002). "Evaluation of whole-body vibration in vehicles." *Journal of Sound and Vibration*, Vol. 253, No. 1, pp. 195-213, DOI: 10.1006/jsvi.2001.4256.

Qin, Y. Y. and Wang H. (2018). "Analytical framework of string stability of connected and autonomous platoons with electronic throttle angle feedback." *Transportmetrica A: Transport Science*, pp. 1-23, DOI: 10.1080/23249935.2018.1518964.

Raimondi, F. M. and Melluso, M. (2008). "Fuzzy motion control strategy for cooperation of multiple automated vehicles with passengers comfort." *Automatica*, Vol. 44, No. 11, pp. 2804-2816, DOI: 10.1016/j.automatica.2008.04.012.

Sau, J., Monteil, J., Billot, R., and El Faouzi, N. E. (2014). "The root locus method: Application to linear stability analysis and design of cooperative car-following models." *Transportmetrica B: Transport Dynamics*, Vol. 2, No. 1, pp. 60-82, DOI: 10.1080/21680566.2014.893416.

Shladover, S. E. (2018). "Connected and automated vehicle systems: introduction and overview." *Journal of Intelligent Transportation Systems*, Vol. 22, No. 3, pp. 190-200, DOI: 10.1080/15472450.2017.1336053.

Shladover, S., Su, D., and Lu, X. Y. (2012). "Impacts of cooperative adaptive cruise control on freeway traffic flow." *Transportation Research Record: Journal of the Transportation Research Board*, Vol. 2324, pp. 63-70, DOI: 10.3141/2324-08.

Sun, J., Zheng, Z., and Sun, J. (2018). "Stability analysis methods and their applicability to car-following models in conventional and connected environments." *Transportation Research Part B: Methodological*, Vol. 109, pp. 212-237, DOI: 10.1016/j.trb.2018.01.013.

Talebpour, A. and Mahmassani, H. S. (2016). "Influence of connected and autonomous vehicles on traffic flow stability and throughput." *Transportation Research Part C: Emerging Technologies*, Vol. 71, pp. 143-163, DOI: 10.1016/j.trc.2016.07.007.

Tang, T. Q., Shi, W., Shang, H., and Wang, Y. (2014). "A new car-following model with consideration of inter-vehicle communication." *Nonlinear Dynamics*, Vol. 76, No. 4, pp. 2017-2023, DOI: 10.1007/s11071-014-1265-9.

Tang, T. Q., Yi, Z. Y., Zhang, J., and Zheng, N. (2017). "Modelling the driving behaviour at a signalised intersection with the information of remaining green time." *IET Intelligent Transport Systems*, Vol. 11, No. 9, pp. 596-603, DOI: 10.1049/iet-its.2017.0191.

Treiber, M., Hennecke, A., and Helbing, D. (2000). "Congested traffic states in empirical observations and microscopic simulations." *Physical Review E*, Vol. 62, No. 2, pp. 1805-1824, DOI: 10.1103/PhysRevE.62.1805.

Vogel, K. (2003). "A comparison of headway and time to collision as safety indicators." *Accident Analysis & Prevention*, Vol. 35, No. 3, pp. 427-433, DOI: 10.1016/S0001-4575(02)00022-2.

Wang, Z., Chen, X. M., Ouyang, Y., and Li, M. (2015). "Emission

mitigation via longitudinal control of intelligent vehicles in a congested platoon." *Computer-Aided Civil and Infrastructure Engineering*, Vol. 30, No. 6, pp. 490-506, DOI: 10.1111/mice.12130.

Wang, H., Wang, W., Chen, J., Xu, C. C., and Li, Y. (2018). "Can we trust the speed-spacing relationship estimated by car-following model from non-stationary trajectory data?" *Transportmetrica A: Transport Science*, pp. 1-23, DOI: 10.1080/23249935.2018.1466211.

Ward, J. A. (2009). *Heterogeneity, lane-changing and instability in traffic: A mathematical approach,* PhD Thesis, University Bristol, Bristol, UK.

Weng, J., Xue, S., Yang, Y., Yan, X., and Qu, X. (2015). "In-depth analysis of drivers' merging behavior and rear-end crash risks in work zone merging areas." *Accident Analysis & Prevention*, Vol. 77, pp. 51-61, DOI: 10.1016/j.aap.2015.02.002.

Wu, Z., Liu, Y., and Pan, G. (2009). "A smart car control model for brake comfort based on car following." *IEEE Transactions on Intelligent Transportation Systems*, Vol. 10, No. 1, pp. 42-46, DOI: 10.1109/TITS.2008.2006777.

Yang, C. D., Ozbay, K., and Ban, X. (2017). "Developments in connected and automated vehicles." *Journal of Intelligent Transportation Systems*, Vol. 21, No. 4, pp. 251-254, DOI: 10.1080/15472450.2017.1337974.

Zhang, H. M. and Kim, T. (2005). "A car-following theory for multiphase vehicular traffic flow." *Transportation Research Part B: Methodological*, Vol. 39, No. 5, pp. 385-399, DOI: 10.1016/j.trb.2004.06.005.